

# Central Blue Clumps in Elliptical Galaxies of the Hubble Ultra Deep Field

Debra Meloy Elmegreen

*Vassar College, Dept. of Physics & Astronomy, Box 745, Poughkeepsie, NY 12604; e-mail: elmegreen@vassar.edu*

Bruce G. Elmegreen

*IBM Research Division, T.J. Watson Research Center, P.O. Box 218, Yorktown Heights, NY 10598, USA; e-mail: bge@watson.ibm.com*

Thomas E. Ferguson

*Vassar College, Dept. of Physics & Astronomy, Box 745, Poughkeepsie, NY 12604; e-mail: thferguson@vassar.edu*

## ABSTRACT

Elliptical galaxies larger than 10 pixels in the Hubble Ultra Deep Field (UDF) were surveyed for internal structure; 30 out of 100 in a sample of 884 morphologically classified galaxies exhibit large blue clumps near their centers. Unsharp-masked images of the best cases are presented. The distributions of the clumps on color-color and color-magnitude diagrams are about the same as the distributions of isolated objects in the UDF field with the same size, suggesting a possible accretion origin. In the few cases where redshifts are published, the clump masses and star-formation ages were determined from stellar evolution models, as were the galaxy masses. The clump mass scales with galaxy mass, probably because of selection effects, and ranges from  $10^6 M_{\odot}$  to  $10^8 M_{\odot}$  for galaxies with masses from  $10^9 M_{\odot}$  to  $10^{11} M_{\odot}$ . The clump star formation age ranges between  $10^7$  yr and  $2 \times 10^8$  yr. With partial evaporation and core contraction in the intervening years, some of these clumps could resemble globular clusters today. Stars that evaporate will contribute to the field population in the elliptical galaxy.

*Subject headings:* galaxies: evolution — galaxies: structure — galaxies: elliptical — galaxies: formation

## 1. Introduction

High resolution images of distant galaxies have revealed many mergers and interactions (e.g., Abraham et al. 1996; Conselice et al. 2003; Conselice 2004; Papovich et al. 2005), as might be expected from hierarchical galaxy build-up (see simulations by Murali et al. 2002). When mergers trigger star formation, the resulting galaxies can be blue and clumpy. Hubble Space Telescope (HST) surveys have confirmed there is a blue population of elliptical galaxies comprising 15% to 30% of the total ellipticals between  $z=0.1$  and 1 (Menanteau et al. 1999; Im et al. 2001; Gebhardt et al. 2003). Color gradients also indicate blue cores and other inhomogeneities in over 30% of resolved ellipticals in the Tadpole field (Menanteau et al. 2004) and in the Hubble Deep Fields North and South (Menanteau, Abraham, & Ellis 2001). Sanchez et al. (2004) found that 25% of the AGN elliptical hosts at redshifts between 0.5 and 1.1 have evidence of central merging. Elliptical galaxies at  $z \sim 0.75$  have star formation time scales less than 1 Gy (Cross et al., 2004). These observations suggest star-formation and galaxy buildup occurs over a wide range of redshifts (Franceschini et al. 1998; Menanteau, Jiminez, & Matteucci 2001).

Nearby elliptical galaxies also suggest a history of mergers and accretions because of internal sub-structure (Redna et al. 2004) and counter-rotating central disks (e.g., Jedrzejewski & Schechter 1988; Carollo et al. 1997; Mehlert et al. 1998; Krajnovic & Jaffe 2004; Morelli et al. 2004). Double nuclei have been reported in several ellipticals (Lauer et al. 1996). Enhanced images sometimes reveal inner spirals or arcs (Lauer et al. 1995) or dust lanes and filaments (Carollo et al. 1997; Elmegreen et al. 2000; Hunt & Malkan 2004). Faber et al. (1999) found that typical elliptical nuclei have a broad range of stellar ages, from 2 to 12 Gy. Marcum, Aars, & Fanelli (2004) examined the colors and profiles of nearby isolated ellipticals and found that some have blue central regions from possible merger events 1-2 Gy ago, even if they show no unusual morphology.

Here we present data on 100 elliptical-like galaxies in the Hubble Ultra Deep Field (UDF), of which 30 show evidence of clumps near their centers in unsharp-masked images.

## 2. Data and Results

The UDF images were observed and processed by Beckwith et al. (2005) and are available on the Space Telescope Science Institute (STScI) archive. The UDF consists of images in 4 filters: F435W (B band, hereafter  $B_{435}$ ; 134880 s exposure), F606W (V band,  $V_{606}$ ; 135320 s), F775W (i band,  $i_{775}$ ; 347110 s), and F850LP (z band,  $z_{850}$ ; 346620 s). The images are 10500 x 10500 pixels with a scale of 0.03 arcsec per px.

We classified all galaxies larger than 10 pixels by eye on the  $i_{775}$  image, making a catalog of 884 objects (Elmegreen et al. 2005). Elliptical galaxies were identified by their optical appearance, contour plots, and radial profiles. Integrated magnitudes were measured in a rectangular box defined by the  $i_{775}$  isophotal contours  $2\sigma$  above the sky noise for each filter (corresponding to a surface brightness of  $26.0 \text{ mag arcsec}^{-2}$ ). The integrated  $i_{775}$ - $z_{850}$  colors of the elliptical galaxies range from  $-0.35$  to  $1.1$ , with an average of  $0.2$  to  $0.3$ . The integrated  $i_{775}$  magnitudes range from  $20.3$  to  $26.5 \text{ mag}$ .

Thirty ellipticals (Table 1) have clumpy structure near their centers. We enhanced these clumps with unsharp-masked techniques by subtracting a 5-pixel Gaussian smoothed image from the originals. Figure 1 shows enhanced images of 8 of them. The figure also shows contour plots on a logarithmic scale, with the lowest contour drawn  $1\sigma$  above sky noise, corresponding to a surface brightness of  $26.8 \text{ mag arcsec}^{-2}$ . In each contour panel, the lower left-hand number represents the horizontal scale of the image in arcsec, and the lower right-hand number is the galaxy identification in the UDF catalog by Beckwith et al., as listed on the STScI website.<sup>1</sup>

In most galaxies, the clumps are randomly oriented in the galaxy with respect to the major axis. Some are very close to the center, and some are partway out in the galaxy. Sometimes bar-like or disk-like central structures are seen (as in UDF25 and UDF9962). These tend to be aligned with the galaxy’s major axis. UDF 2162 shows a ring with three embedded clumps near the nucleus. UDF900 has an inner spiral with several clumps along the spiral arms (reminiscent of the spiral in IC 3328 – Jerjen, Kalnajs, & Binggeli 2000).

Figure 2 shows how a typical elliptical, UDF900, appears featureless on a normal grayscale image. The radial profile from ellipse fits is either a de Vaucouleurs  $r^{1/4}$  law or a double power (Sersic) law. For the double power law, the inner slope is  $-0.6$  and the outer is steeper,  $-2.4$ , as in a “core” galaxy (Trujillo et al. 2004). The galaxy’s position angle and ellipticity are shown as a function of radius; the spiral appears as an abrupt change near the center.

The colors and magnitudes of clumps in each galaxy in Table 1 were measured by photometry on a box encompassing the peaks, typically 3-5 px across. We subtracted the underlying galaxy intensity from the clump intensity by measuring the featureless regions adjacent to each clump. This background subtraction typically made the clumps  $0.1 \text{ mag}$  bluer in  $i_{775} - z_{850}$  and  $0.4 \text{ mag}$  dimmer in  $i_{775}$ . The measuring errors are about  $0.1 \text{ mag}$  for the UDF images. Figure 3 (top left) plots  $B_{435}$ - $V_{606}$  versus  $i_{775} - z_{850}$  for the clumps and nuclei of the galaxies in Table 1, and for all 100 elliptical galaxies in integrated light.

---

<sup>1</sup>[http://archive.stsci.edu/pub/hlsp/udf/acs-wfc/h\\_udf\\_wfc\\_VI\\_L\\_cat.txt](http://archive.stsci.edu/pub/hlsp/udf/acs-wfc/h_udf_wfc_VI_L_cat.txt)

For each galaxy, the integrated colors are redder than the clumps by several tenths of a magnitude. In some galaxies the nuclei are blue in  $i_{775-z850}$ . Figure 3 (bottom left) shows  $i_{775}$  versus  $i_{775} - z_{850}$  for the clumps and the integrated galaxies. The large spread in color for clumps fainter than  $i_{775} \sim 30$  mag is probably the result of low signal-to-noise. The clumps average  $\sim 4$  mag fainter than the integrated galaxies.

If the clumps in these elliptical galaxies have been accreted, then the field should contain isolated objects that are similar in color and magnitude. The right hand side of Figure 3 shows sources in the UDF catalog that have sizes between 3 and 4 pixels FWHM. This is approximately the size range for the clumps in our elliptical galaxy sample. The color-magnitude and color-color distributions of the tiny field clumps resemble the distributions for the elliptical galaxy clumps, lending credibility to the accretion model.

The redshifts of four of our clumpy ellipticals were measured by Vanzella et al. (2004) and are listed in Table 2. They range from  $z = 0.218$  to  $1.317$ , illustrating how clump formation or accretion occurs during a wide range of epochs. The same survey found the redshifts of 2 other ellipticals that do not have obvious clumps, UDF 3088 and UDF 9264. Using these redshifts, we converted the apparent magnitudes into absolute  $i_{775}$  AB magnitudes and obtained the major axis galaxy diameters, considering a standard  $\Lambda = 0.7$  cosmology. The background-subtracted  $B_{435}-V_{606}$ ,  $V_{606}-i_{775}$ , and  $i_{775}-z_{850}$  colors and the  $i_{775}$ -band magnitudes of the clumps and whole galaxies were also compared to Bruzual & Charlot (2003) evolution models in order to estimate the masses, ages, and star formation decay times, assuming an exponential star formation rate. Two values of the internal dust extinction were taken, one from Rowan-Robinson (2003) for the appropriate redshifts and another four times larger for comparison. The Rowan-Robinson extinctions are slightly lower than others measured for spirals at the same redshift (Adelberger & Steidel 2000; Papovich, Dickinson, & Ferguson 2001), but they may be a good approximation for ellipticals; the second case with  $4\times$  higher values should bracket most previous results. Absorption from intervening hydrogen lines and continuum were included, from Madau (1995). The models are discussed in Elmegreen & Elmegreen (2005).

The model results are in Table 2. The clump masses range from  $6 \times 10^5 M_{\odot}$  to  $5 \times 10^7 M_{\odot}$ , with slightly larger values for higher extinctions (as shown in parentheses). The star formation ages of the clumps are typically  $\sim 10^8$  yr for low extinction and several  $\times 10^7$  yr for high extinction. Clump diameters are several hundred pc to a kpc. Only clumps that gave close fits to the model colors (with an rms deviation from all 3 colors less than several tenths) are listed with a mass and age. For the whole galaxies, the star formation ages are much longer than for the clumps, but still less than the age of the Universe at that redshift. This suggests the ellipticals either have lingering star formation or contain other, more dissolved,

clumps spanning a wide range of ages. To give an upper limit to the whole galaxy mass, solutions were also found for assumed ages equal to the galaxy age if star formation started at  $z = 6$  and then decayed exponentially. In these cases, the decay time was chosen to match the colors. These results are given in square brackets. Typically the galaxy mass increases by a factor of  $\sim 3$  with this assumption. Considering the large measurement and model uncertainties, these results should be viewed as order of magnitude estimates.

The clump ages appear to be comparable to or less than the orbital accretion times for the elliptical galaxies, which typically exceed several hundred My. This implies that most of the young stars formed after the clumps entered the galaxies, if the accretion model is correct. We note from Figure 3 that the elliptical galaxy clumps lie at the lower envelope of the field clump  $B_{435}$ - $V_{606}$  color distribution, consistent with triggered star formation during accretion. Alternatively, the clumps could have formed inside gas clouds that were already in the ellipticals.

The clump masses are an order of magnitude larger than globular cluster masses. Considering the likely evaporation of cluster stars in the intervening time and the likely central concentration of young stars inside these clumps, some of these objects could turn into globular clusters. This situation slightly resembles models where globular clusters and ellipticals both form during gas-rich mergers (e.g., Ashman & Zepf 1992). However, the clumps here are younger than the relaxation times of the host galaxies, so if they formed when the ellipticals formed, then star formation had to continue for a relatively long time. The observations more resemble models where globular clusters enter a galaxy as parts of dwarf galaxies (e.g., Searle & Zinn 1978). If the observed clumps evaporate more completely, then the elliptical galaxies will become more smooth, leaving only faint remnants of accretion such as those discussed in the introduction.

We are grateful to Vassar College for undergraduate research support for T.E.F. and for support from the Salmon fund for D.M.E.. B.G.E. is supported by the National Science Foundation through grant AST-0205097.

## REFERENCES

- Abraham, R., Tanvir, N., Santiago, B., Ellis, R., Glazebrook, K., & van den Bergh, S. 1996, MNRAS, 279, L47
- Adelberger, K.L., & Steidel, C.C. 2000, ApJ, 544, 218
- Ashman, K.M., & Zepf, S.E. 1992, ApJ, 384, 50
- Beckwith, S.V.W. et al., 2005, in preparation
- Bruzual, G. & Charlot, S. 2003, MNRAS, 344, 1000
- Carollo, C., Franx, M., Illingworth, G., & Forbes, D. 1997, ApJ, 481, 710
- Conselice, C. 2004, astro-ph/0405102
- Conselice, C., Bershadsky, M., Dickinson, M., & Papovich, C. 2003, AJ, 126, 1183
- Cross, N.J.G., et al. 2004, AJ, 128, 1990
- Elmegreen, B., & Elmegreen, D. 2005, submitted to ApJ
- Elmegreen, D., Elmegreen, B., Chromey, F., & Fine, M. 2000, AJ, 120, 733
- Elmegreen, D., Elmegreen, B., Rubin, D., & Schaffer, M. 2005, in preparation
- Faber, S., Trager, S., Gonzalez, J., & Worthey, G. 1999, Ap&SS, 267, 273
- Franceschini, A., Silva, L., Fasano, G., Granato, G.L., Bressan, A., Arnouts, S., Danese, L. 1998, ApJ, 506, 600
- Gebhardt, K., et al. 2003, ApJ, 597, 239
- Hunt, L., & Malkan, M. 2004, ApJ, 616, 707
- Im, M., et al. 2001, AJ, 122, 750
- Jedrzejewski, R., & Schechter, P. 1988, ApJ, L330
- Jerjen, H., Kalnajs, A., & Binggeli, B. 2000, A&A, 358, 845
- Krajinovic, D., & Jaffe, W. 2004, A&A, 428, 877
- Lauer, T. et al. 1995, AJ, 110, 2622
- Lauer, T. et al. 1996, ApJ, 471, L79

- Madau, P. 1995, *ApJ*, 441, 18
- Marcum, P., Aars, C., & Fanelli, M. 2004, *AJ*, 127, 3213
- Mehlert, D., Saglia, R., Bender, R., & Wegner, G. 1998, *MNRAS*, 332, 33
- Menanteau, F., Abraham, R., & Ellis, R. 2001, *MNRAS*, 322, 1
- Menanteau, F., Ellis, R., Abraham, R., Barger, A., & Cowie, L. 1999, *MNRAS*, 309, 208
- Menanteau, F., Jiminez, R., & Matteucci, F. 2001, *ApJ*, 562, L23
- Menanteau, F., et al. 2004, *ApJ*, 612, 202
- Morelli, L., Halliday, C., Corsini, E., Pizzella, A., Thomas, D., Davies, R., Bender, R., Birkinshaw, M., & Bertola, F. 2004, *MNRAS*, 354, 753
- Murali, C., Katz, N., Hernquist, L., Weinberg, D., & Dave, R. 2002, *ApJ*, 571, 1
- Papovich, C., Dickinson, M., & Ferguson, H.C. 2001, *ApJ*, 559, 620
- Papovich, C., Dickinson, M., Giavalisco, M., Conselice, C., & Ferguson, H. 2005, *astro-ph/0501088*
- Redna, F., Forbes, D., Beasley, M., O’Sullivan, E., & Goudfrooij, P. 2004, *MNRAS*, 354, 851
- Rowan-Robinson, M. 2003, *MNRAS*, 345, 819
- Sanchez, S. et al., 2004, *ApJ*, 614, 586
- Searle, L. & Zinn, R. 1978, *ApJ*, 225, 357
- Trujillo, I., Erwin, P., Ramos, A., & Graham, A. 2004, *AJ*, 127, 1917
- Vanzella, E., Cristiani, S., Dickinson, M., Kuntschner, H., Moustakas, L. A., Nonino, M., Rosati, P., Stern, D., Cesarsky, C., Ettori, S., and 7 coauthors, 2004, *astro-ph/0406591*

Table 1. Elliptical Galaxies with Clumps

UDF no.	Features	UDF no.	Features
25	central bar; 5 nearby clumps	3174	2 outer clumps
100	3 near-nuclear clumps	3677	elongated nucleus
153	1 near-nuclear clump, 1 mid-disk clump	4142	elongated nucleus plus 1 near-nuclear clump
206	1 near-nuclear clump	4389	central arc plus 2 clumps
221	4 near-nuclear clumps	4445	1 nuclear clump, outer streamers
703	2 near-nuclear clumps	4551	elongated nucleus
900	central spiral with 10 clumps	6018	lumpy nucleus plus 1 nuclear clump
901	3 nuclear clumps plus 3 clumps outside nucleus	6027	2 near-nuclear clumps plus 2 outer clump arcs
1088	nuclear clump plus 2 outer clumps	6288	2 big nuclear clumps plus 3 smaller clumps
1564	1 near-nuclear clump plus 2 outer clumps	8138	2 nuclear clumps
1607	elongated lumpy nucleus	8680	elongated nucleus
1727	elongated nucleus	9962	nuclear bar; 2 end-of-bar clumps
1960	2 near-nuclear arcs	E1 <sup>a</sup>	1 near-nuclear clump
2162	nuclear arc with 3 clumps	E2 <sup>a</sup>	1 nuclear clump plus 1 outer arc
2974	1 near-nuclear clump	E3 <sup>a</sup>	elongated nucleus plus 1 near-nuclear clump

<sup>a</sup>no UDF numbers are given for three object in our table; we designate them by E1, E2, and E3. Their coordinates are, E1: 3<sup>h</sup>32<sup>m</sup>30.4637<sup>s</sup>, -27°48′3.068″; E2: 3<sup>h</sup>32<sup>m</sup>42.5604<sup>s</sup>, -27°45′50.196″; E3: 3<sup>h</sup>32<sup>m</sup>42.2572<sup>s</sup>, -27°49′15.137″

Table 2. Properties for Galaxies with Spectroscopic Redshifts

Object	$z^a$	i mag	B-V mag	V-i mag	i-z mag	I mag	Diam. kpc	Age Fit <sup>b</sup> My	Age Max <sup>c</sup> My	log Mass <sup>b</sup> $M_{\odot}$	log Mass Max <sup>c</sup> $M_{\odot}$
UDF 153	0.98	21.59	2.05	1.45	0.88	-22.5	29	1900(1900)	5100	11.1(11.8)	11.6(12.2)
Clump 1		28.53	1.03	0.48	0.08	-15.5	0.8	180(40)		7.3(7.5)	
Clump 2		26.67	0.80	0.21	-0.16	-17.4	1.7	90(14)		7.7(7.8)	
UDF 3088	0.127	25.94	1.37	1.02	0.73	-13.0	1.6	4800(1300)	11000	7.1(7.1)	7.4(7.4)
UDF 4142	0.737	21.70	0.60	0.66	0.20	-21.6	15	120(50)	6200	9.5(9.7)	10.3(11.0)
Clump 1		29.06	-0.05	0.10	0.67	-14.2	0.8	13(10)		5.8(6.4)	
UDF 6027	1.317	23.80	1.12	1.23	0.91	-21.1	16	1000(700)	3900	10.5(11.1)	10.8(11.5)
Clump 1		30.21	-0.16	0.03	-0.21	-14.7	1.0	20( ... )		6.0( ... )	
Clump 2		30.87	6.26	0.84	-0.35	-14.0	0.9	...		...	
Clump 3		31.06	-2.54	3.23	-0.03	-13.8	1.1	...		...	
Clump 4		30.08	-0.00	-0.46	-1.77	-14.8	1.4	...		...	
UDF 9264	1.096	21.96	1.94	1.53	1.08	-22.4	32	1900(1300)	4600	11.2(11.8)	11.6(12.2)
E2	0.218	22.36	0.28	1.04	0.18	-17.8	6	1200(45)	10000	8.4(8.3)	8.9(9.4)
Clump 1		27.75	...	...	-0.26	-12.4	0.4	...		...	

<sup>a</sup>Redshifts from Vanzella et al. (2004)

<sup>b</sup>Values in parentheses are for  $4\times$  the extinction compared to Rowan-Robinson (2003).

<sup>c</sup>Values are best fits assuming star formation began at redshift  $z = 6$ .

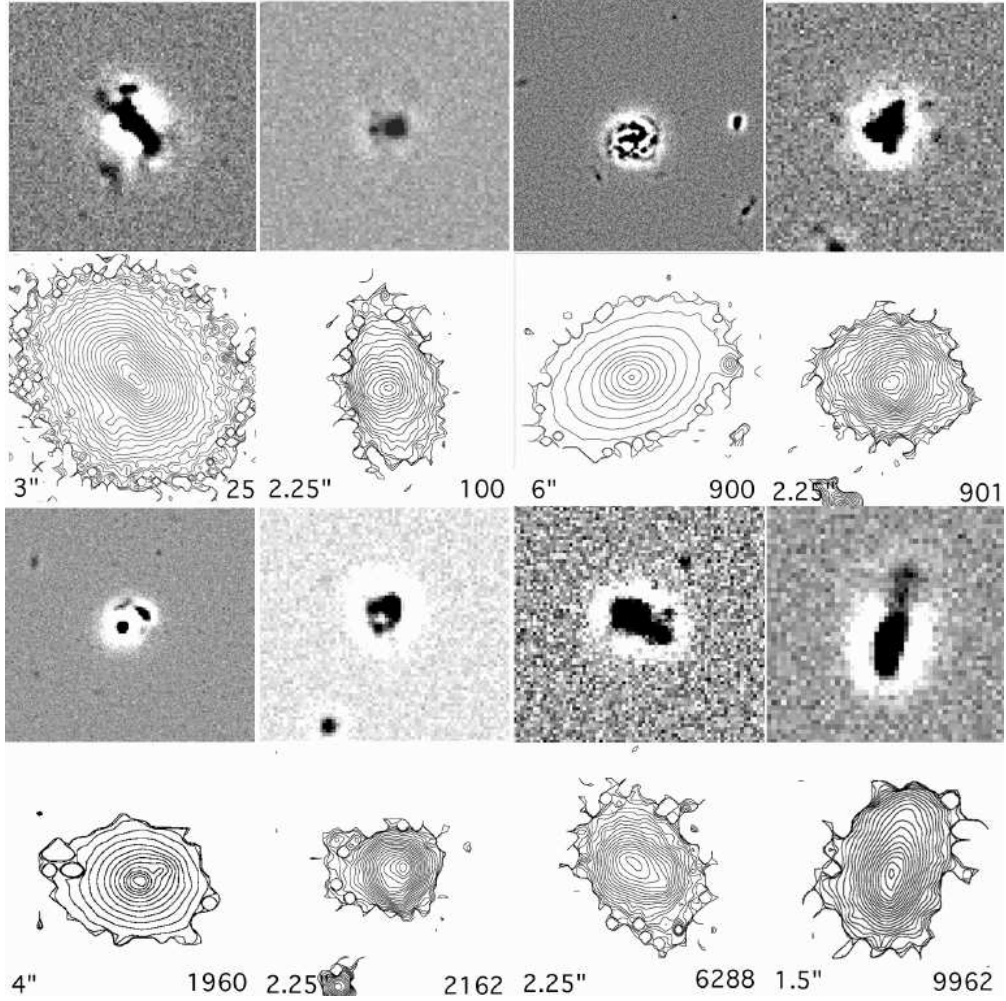


Fig. 1.— Unsharp-masked  $i_{775}$  images and logarithmic contour plots are shown for 8 of the 30 galaxies in Table 1, which have central clumpy features.

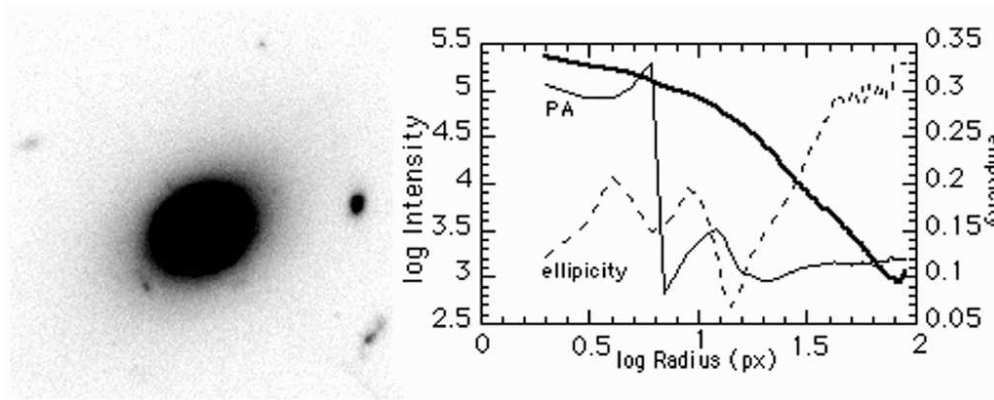


Fig. 2.— The  $i_{775}$  grayscale image of UDF 900 is shown with the mean intensity, position angle, and ellipticity as a function of radius, based on ellipse fits. The spiral structure evident in Figure 1 ends at a radius of about 30 pixels.

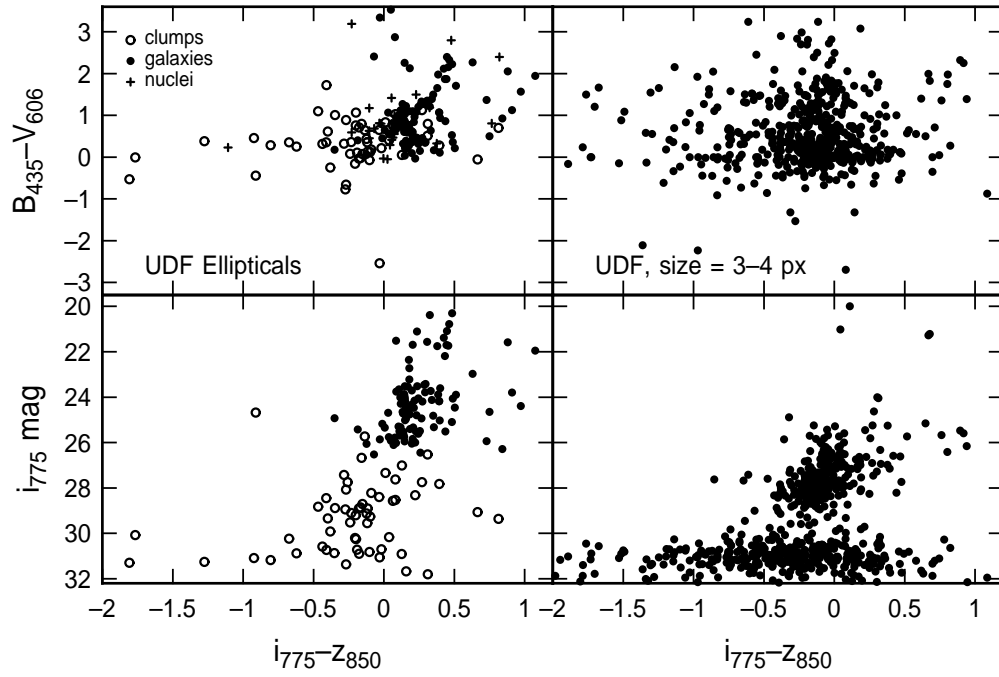


Fig. 3.— Top left: Color-color distributions of the clumps and nuclei for galaxies in Table 1, and for all 100 elliptical galaxies in integrated light. Bottom left: Color-magnitude distributions of the clumps (open circles) and integrated elliptical galaxies (dots). Right: Similar distributions for all UDF-catalogued objects with FWHM between 3 and 4 px.